Aggregation of Puroindoline in Phospholipid Monolayers Spread at the Air-Liquid Interface

L. Dubreil,* V. Vié,* S. Beaufils,* D. Marion,† and A. Renault*
*Groupe Matière Condensée et Matériaux, Université de Rennes, Campus Beaulieu, Rennes, France; and †Unité de Recherche sur les Protéines Végétales et leurs Interactions, Institut National de la Recherche Agronomique, Nantes, France

ABSTRACT Puroindolines, cationic and cystine-rich low molecular weight lipid binding proteins from wheat seeds, display unique foaming properties and antimicrobial activity. To unravel the mechanism involved in these properties, the interaction of puroindoline-a (PIN-a) with dipalmitoylphosphatidylcholine (DPPC) and dipalmitoylphosphatidylglycerol (DPPG) monolayers was studied by coupling Langmuir-Blodgett and imaging techniques. Compression isotherms of PIN-a/phospholipid monolayers and adsorption of PIN-a to lipid monolayers showed that the protein interacted strongly with phospholipids, especially with the anionic DPPG. The electrostatic contribution led to the formation of a highly stable lipoprotein monolayer. Confocal laser scanning microscopy and atomic force microscopy showed that PIN-a was mainly inserted in the liquid-expanded phase of the DPPC, where it formed an aggregated protein network and induced the fusion of liquid-condensed domains. For DPPG, the protein partitioned in both the liquid-expanded and liquid-condensed phases, where it was aggregated. The extent of protein aggregation was related both to the physical state of phospholipids, i.e., condensed or expanded, and to the electrostatic interactions between lipids and PIN-a. Aggregation of PIN-a at air-liquid and lipid interfaces could account for the biological and technological properties of this wheat lipid binding protein.

INTRODUCTION

Cereal lipid binding proteins have been extensively studied in recent years for both their unique role in seed physiology as well as for their potential applications in plant breeding and food processing of crops (Marion and Clark, 1995; Douliez et al., 2000). Among wheat lipid binding proteins, puroindolines form a major family of proteins from seed endosperm that are isolated by Triton X-114 phase partitioning like transmembrane proteins (Blochet et al., 1993). Puroindolines are composed of two major proteins with a molecular mass ~13 kDa, puroindoline-a (PIN-a) and puroindoline-b (PIN-b). PIN-a contains 115 amino-acid residues with five disulfide bridges and displays an unique tryptophan-rich domain (Trp-Arg-Trp-Trp-Lys-Trp-Trp-Lys). The amino-acid sequences of PIN-a and PIN-b display ~60% homology, but the tryptophan-rich domain of PIN-b is slightly truncated (Trp-Pro-Thr-Trp-Trp-Lys). Some similarities have been highlighted between the primary and secondary structures of plant nonspecific lipid transfer proteins (ns-LTP) and puroindolines (Le Bihan et al., 1996), which suggests that ns-LTP and puroindoline three-dimensional structures are closely related (Douliez et al., 2000).

The biological role of puroindolines is unknown. It has been suggested that these proteins could play a major role in the texture of wheat endosperm by controlling the interactions between the starch granules and the protein matrix. This interaction involves the formation of a lipid-protein interface where puroindolines could play a key role (Morris, 2002). Furthermore, it has been shown, in vitro, that puroindolines display antifungal properties. Especially a synergistic antifungal effect has been highlighted in presence of purothionin, an antifungal protein of wheat seeds (Dubreil et al., 1998a). Furthermore, it has been shown that the transfer of puroindoline genes in rice enhances fungal disease resistance of this cereal plant that does not normally contain such proteins (Krishnamurthy et al., 2001). The antimicrobial properties of puroindolines are probably related to their capability of disturbing membrane permeability (Mattei et al., 1998; Charnet et al., 2003). All these experiments strengthen a role of puroindolines in the defense of plants against their microbial pathogens.

Interfacial and lipid binding properties of puroindolines represented also a great interest in food processing. Puroindolines adsorb rapidly at air-liquid interfaces where they form stable films responsible for the high foaming properties of these wheat proteins (Biswas et al., 2001a,b). Interestingly, puroindolines are capable of preventing the destabilization of protein foams by lipids (Clark et al., 1994; Husband et al., 1994) while some puroindoline-surfactant and puroindoline-phospholipid complexes can exhibit higher foaming properties than the isolated protein (Wilde et al., 1993; Dubreil et al., 1997). It has been shown that puroindolines play a major role in the formation and expansion of the gas cell in bread dough (Dubreil et al., 1998b). By confocal scanning laser microscopy, it was shown that puroindolines display, as detergents, a defatting effect that prevents, in bread doughs, gas bubbles from coalescence and film rupture by lipid aggregates and oil droplets (Dubreil et al., 2002).

Both biological and technological properties of puroindolines are mainly related to their interaction with lipid

Submitted May 22, 2003, and accepted for publication July 7, 2003.

Address reprint requests to Laurence Dubreil, Institut National de la Recherche sur les Protéines Végétales et Leurs Interactions, rue de la Géraudière, B.P. 71 627, F-44316 Nantes Cedex 3. Tel.: 33-024-067-50-56; Fax: 33-024-067-50-25; E-mail: laurence.dubreil@wanadoo.fr.

0006-3495/03/10/2650/11 $2.00

interfaces. Therefore, to determine the mechanisms related to the interfacial properties of puroindolines, we have studied the effect of PIN-a, the major protein of this protein family, on the structure and organization of phospholipid monolayers by coupling Langmuir-Blodgett and imaging techniques, i.e., confocal scanning laser microscopy (CLSM) and atomic force microscopy (AFM). Lipid and lipid-protein monolayers have been widely used for investigating mechanisms occurring in biological membranes and are obviously pertinent for mimicking the films that stabilize gas bubbles (Brockman, 1999; Maget-Dana, 1999). The composition as well as the physical state of these monolayers can be easily controlled. The monolayers formed at air-liquid interfaces can be transferred to solid support with minimal perturbation to study their structure and organization at the micron and nanometer scales by fluorescence and atomic force microscopy, respectively (Hollars and Dunn, 1998; Vié et al., 2000). Two model synthetic phospholipids were used, the zwitterionic DPPC and the anionic DPPG to highlight the impact of electrostatic interactions on the formation and structure of puroindoline-phospholipid monolayers.

MATERIALS AND METHODS

Materials

665/676, $C_{29}H_{23}BF_2N_2$, (*E*, *E*)-3,5-*bis*-(4-phenyl-1,3-butadienyl)-4,4-difluoro-4-bora-3a,4a-diaza-*s*-indacene (BODIPY), and 555/580, $C_{29}H_{25}N_3O_7$, 5-carboxytetramethyl-rhodamine, succinimidylester (5-TAMRA), were provided by Molecular Probes (Eugene, OR). A solution of BODIPY (1 mg/ml) in chloroform was prepared and stored in the dark at −20°C. L-α-dipalmitoylphosphatidylcholine (DPPC) and L-α-dipalmitoyl-phosphatidyl-*dl*-glycerol (DPPG) were purchased from Avanti Polar Lipids (Alabaster, AL) and were used without further purification. DPPC and DPPG stock solutions (2 mg/ml) were prepared in chloroform and in chloroform/methanol 4:1 (v:v), respectively, and stored at −20°C under nitrogen. PIN-a was isolated and purified using Triton X-114 phase partitioning and chromatographic techniques as previously described (Dubreil et al., 1997). The purity of PIN-a was checked by reversed-phase high performance liquid chromatography (HPLC) and mass spectrometry.

PIN-a was conjugated with the 5-TAMRA succinimidylester as described by the manufacturer (Molecular Probes). Briefly, 10 mg of PIN-a were solubilized in 2 ml of 0.1 M sodium bicarbonate buffer, pH 8.3. The 5-TAMRA succinimidylester was dissolved in DMSO at 10 mg/ml just before starting the reaction. The reactive dye solution (50 μl) was slowly added to the protein solution and the reaction was incubated in dark for 1 h at room temperature with continuous stirring. The reaction was stopped by adding 0.1 ml of freshly prepared 1.5 M hydroxylamine, pH 8.5. The hydroxylamine was incubated for 1 h at room temperature to remove unstable dye conjugates. Labeled PIN-a (rho-PIN-a) was separated from unreacted reagent by extensive dialysis against distilled water and this separation was followed by spectrofluorimetry. Purity of the rho-PIN-a was checked by C4 reversed-phase HPLC. The efficiency of labeling reaction was determined by measuring the absorbance of the protein at 280 nm (A_{280}) and the absorbance of the 5-TAMRA dye (A_{555}) at its maximum wavelength ($\lambda_{max} = 555$ nm).

The protein concentration of the protein conjugate and the degree of labeling were calculated from the following equations according to the instructions of the manufacturer.

$$protein\,concentration\,(M) = \frac{A_{280}[-(A_{555} \times 0.30)]}{\in_{protein}} \times dilution\,factor, \quad (1)$$

where ε is the molar extinction coefficient of PIN-a and 0.30 is a correction factor to account for absorption of the dye at 280 nm.

The degree of labeling was calculated from Eq. 2,

$$Mol\,of\,dye\,per\,mol\,of\,protein = n = \frac{A_{555} \times dilution\,factor}{65{,}000 \times protein\,concentration\,(M)}, \quad (2)$$

where 65,000 is the approximate molar extinction coefficient of the 5-TAMRA, SE dye at 555 nm.

The surface activity of the labeled PIN-a (rho-PIN-a) depended on the extent of labeling. In our conditions of labeling, one molecule of 5-TAMRA was bound per molecule of PIN-a ($n = 1$) and we have checked that the surface activity of rho-PIN-a and PIN-a were identical.

Methods

Monolayer and Langmuir-Blodgett techniques

The surface pressure-area isotherms were obtained by means of a computer-controlled and user-programmable Langmuir Teflon-coated trough (KSV5000, equipped with a single movable barrier of total surface area 0.0724 m^2). The surface pressure was measured following a Wilhelmy-plate method using a roughened platinum plate connected to a microelectronic feedback system for surface pressure measurement. Before starting the experiment, the trough was cleaned successively with deionized water, ethanol, and finally with ultrapure deionized water (UHQ ELGA, Vivendi Water Systems, France). The phosphate buffer (0.01 M phosphate, 0.1 M NaCl, pH 7.2) forming the subphase in the Langmuir film balance experiments was prepared in ultrapure water. The trough was filled up by the buffer and before each experiment, surface active impurities were removed by simultaneous sweeping and suction of the interface. For mixed monolayers, the protein and then the lipid solution were spread on the aqueous subphase using a high precision Hamilton microsyringe. It was checked that the amount of organic solvent used in these experiments does not change the shape of the protein isotherm. To ensure complete mixing of the film components at the interface and allow sufficient equilibration, monolayers at air-buffer interface were rested 5 h before a compression at 3 cm/min. The trough was thermostated by a water circulating bath at a temperature of 20°C. Each experiment was repeated at least 3×.

For adsorption of PIN-a to lipid monolayers, the phospholipid stock solution was gently deposited at the air-buffer interface with a microsyringe. After 10 min to allow evaporation of the solvent, films were compressed by moving the barrier at a rate of 3 cm/min and equilibrated during 3 h to the desired surface pressure. Then, the PIN-a solution (0.1 ml of 2 mg/ml in buffer) was injected into the subphase just beneath the phospholipid monolayer from the opposite side of the barrier. The increase of surface pressure due to adsorption of the protein to the monolayer was recorded automatically as function of time with a computer. The isotherms presented were the average of three experimental runs, which were reproducible within a standard deviation of 0.2 mN/m.

Phospholipid and phospholipid-PIN-a monolayers were deposited at constant surface pressure onto mica for AFM and CLSM studies. To visualize the localization of fluid phase and PIN-a by CLSM, BODIPY, and rho-PIN-a, were added to a final concentration of 5 mol % to phospholipid and protein solutions, respectively. The labeled molecules were spread at the air-water interface and after an equilibration period of 10 min, lipid, protein, or lipid-protein monolayers were compressed to the desired surface pressure. After an equilibration period of ~3 h, transfer was performed by pulling

freshly cleaved mica through the air-water interface at a rate of 1 mm/min under constant surface pressure.

Confocal laser scanning microscopy (CLSM)

The lipid films deposited onto mica were imaged with an inverted Zeiss LSM 410 Axiovert microscope. CLSM was used with the appropriate laser excitation and filters for each fluorescent probe. Rho-PIN-a was excited by the 543-nm line of the green He-Ne laser with a long pass at 570 nm, and BODIPY was excited by the 633-nm line of the He-Ne laser with a long pass at 665 nm.

Atomic force microscopy

Surface images of the Langmuir-Blodgett monolayers were obtained under ambient conditions using a Pico-plus atomic force microscope (Molecular Imaging, Phoenix, AZ) operating in contact mode and acoustic ACt mode. Two scanners of 100 μm and 10 μm were used for measurements. Topographic images were acquired in constant force mode using silicone nitride tips with nominal spring constant of 60 mN/m. Either triplicate samples were prepared for each monolayer composition and at least five separate areas were imaged for each sample.

RESULTS

Isothermal compression of mixed PIN-a/DPPC and PIN-a/DPPG monolayers

Fig. 1 *A* reported compression isotherms of lipid (*DPPC curve 1*), protein (*PIN-a curve 10*), and mixed lipid-protein monolayers (PIN-a /DPPC with increasing PIN-a concentration, *curves 2–9*).

At a surface pressure of 4.5 mN/m, the DPPC pressure area (π-A) isotherm (*curve 1*) exhibited a typical LE-LC phase transition evidenced by a plateau in the π-A isotherm as previously observed (Disher et al., 1999; Minones et al., 2002). Contrary to DPPC, the PIN-a isotherm (*curve 10*) was quite expanded with a characteristic plateau at $\pi = 12.5$ mN/m. The mixed PIN-a/DPPC monolayer exhibited an intermediate behavior compared with what it was displayed by single protein and lipid components. Even at very low concentration, the presence of PIN-a strongly affected the shape of the compression isotherm. As the PIN-a concentration increased, the typical plateau observed for pure DPPC gradually disappeared and the LE-LC phase transition was shifted to higher surface pressure, 6 mN/m for a molar protein fraction $X_{\text{PIN-a}} = 0.09$, (*curve 4*). From $X_{\text{PIN-a}} = 0.055$ (*curve 3*), the π-A isotherms for the mixed PIN-a/DPPC exhibited an inflection point similar to the plateau curve for pure PIN-a at a surface pressure of 12.5 mN/m. A third inflection point was observed at a surface pressure of 30 mN/m from $X_{\text{PIN-a}} = 0.055$ (*curve 3*) to $X_{\text{PIN-a}} = 0.125$ (*curve 5*). Above 35 mN/m, the isotherms of the mixed lipid-protein monolayers coincided with that of pure DPPC.

The inset of Fig. 1 *A* (*curves 6–10*) shows compression isotherms of DPPC/PIN-a mixed monolayers with higher PIN-a content, i.e., >12.5 mol %. At these higher $X_{\text{PIN-a}}$, the

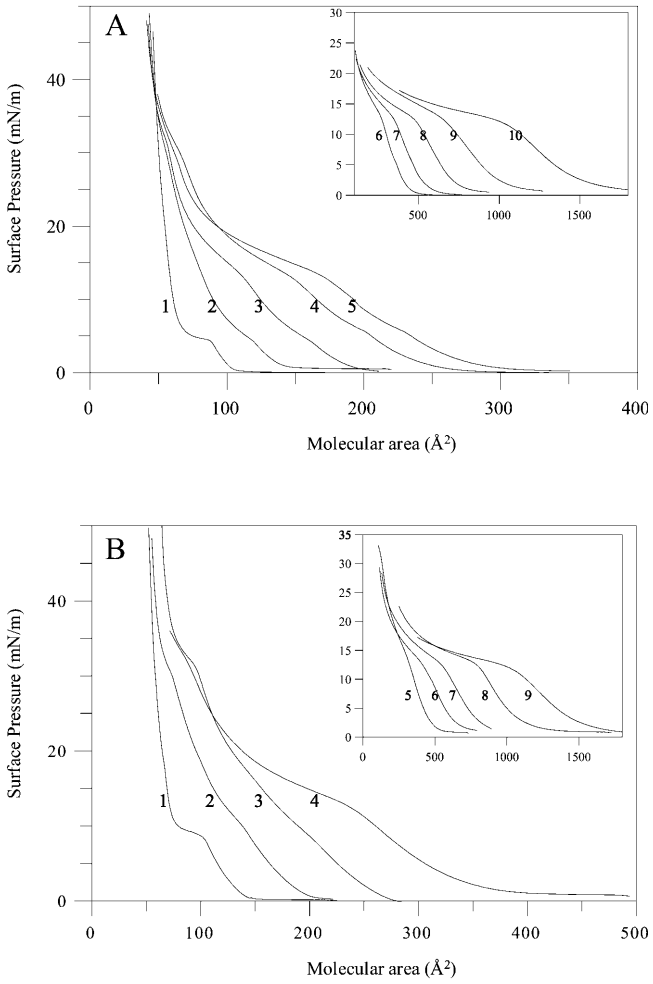

FIGURE 1 (*A*) π-A Langmuir isotherms of DPPC (*curve 1*), PIN-a (*curve 10*), and PIN-a/DPPC monolayers (at increasing PIN-a concentration from *curves 2–9*) spread on buffer subphase (0.01 M phosphate buffer, 0.1 M NaCl, pH 7,4) at 20°C. Curves 1–10 correspond to PIN-a molar fractions of (*1*) 0, (*2*) 0.014, (*3*) 0.055, (*4*) 0.09, (*5*) 0.125, (*6*) 0.185, (*7*) 0.33, (*8*) 0.5, (*9*) 0.66, and (*10*) 1, respectively. (*B*) π-A isotherms for DPPG, PIN-a, and PIN-a /DPPG monolayers (see Fig. 1 *A* for experimental conditions). Curves 1–9 correspond to PIN-a concentration in molar fraction of (*1*) 0, (*2*) 0.014, (*3*) 0.055, (*4*) 0.125, (*5*) 0.185, (*6*) 0.33, (*7*) 0.5, (*8*) 0.66, and (*9*) 1, respectively.

π-A isotherms resembled those of pure PIN-a isotherm. As the PIN-a concentration increased, the curves were gradually shifted toward higher values of mean molecular area and from $X_{\text{PIN-a}} = 0.33$ (*curve 7*), the typical inflection point of DPPC totally disappeared. The interaction between PIN-a and DPPC at the air-water interface can be examined by plotting the mean molecular area of the mixed monolayer as a function of the molar fraction of PIN-a. Fig. 2 shows such a plot at a surface pressure of 15 mN/m. Theoretical values of molecular area were calculated on the basis of an additive relation (Gaines, 1966). In the ideal case, the mean molecular area displayed a linear behavior versus PIN-a molar fraction (*dotted line* in Fig. 2, for DPPC). A positive deviation from linearity was observed from $X_{\text{PIN-a}} = 0.09$ to $X_{\text{PIN-a}} = 0.66$,

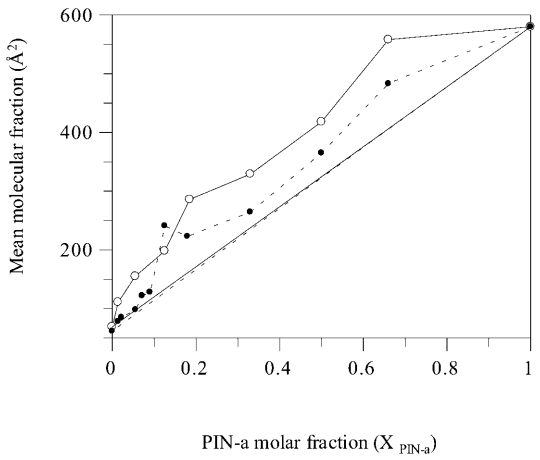

FIGURE 2 Influence of mole fraction of PIN-a (X_{PIN-a}) on the mean molecular area, A, of PIN-a/DPPC, and PIN-a/DPPG monolayers spread on the phosphate buffer subphase. Ideal mixing (—) and experimental data (- -●- -) for PIN-a/DPPC monolayers; ideal mixing (- - -) and experimental data (—○—) for PIN-a/DPPG monolayers.

suggesting a nonideal mixing of the components in the film. The maximal positive deviation from ideal mixing was observed at $X_{PIN-a} = 0.125$, where it was almost 2× higher than the ideal value.

Fig. 1 *B* shows experimental π-A isotherms of DPPG and DPPG-PIN-a films. As shown in Fig. 1 *B* (*curve 1*), the typical LE-LC phase transition of DPPG took place at ~10 mN/m, in agreement with previously reported values (Subirade et al., 1995). As for PIN-a/DPPC monolayers, the mixed monolayers of PIN-a and DPPG (*curves 2–8*) exhibited an intermediate behavior compared with what it was observed for single lipid, $X_{PIN-a} = 0$, i.e., pure DPPG (*curve 1*) and protein, $X_{PIN-a} = 1$, i.e., pure PIN-a, (*curve 9*) components. Fig. 1 *B* shows that, even at low PIN-a content $X_{PIN-a} = 0.014$ (*curve 2*), the shape of the DPPG isotherm was highly affected with a gradual disappearance of the typical plateau displayed by the pure DPPG at 10 mN/m. From $X_{PIN-a} = 0.014$ (*curve 2*), an inflection point at 30 mN/m was observed for the mixed PIN-a/DPPG π-A isotherms. In contrast with the mixed DPPC/PIN-a monolayer, it was observed that, at 35 mN/m, the molecular area of the DPPG/PIN-a monolayer was higher than the molecular area of the pure DPPG.

Mean molecular area for mixed PIN-a/DPPG monolayers was plotted versus the molar fraction of PIN-a. A positive deviation from linearity (*straight line*) was observed between $X_{PIN-a} = 0.014$ and $X_{PIN-a} = 0.66$ (see Fig. 2). It was worthy to note that, in the case of DPPG/PIN-a monolayers, the positive deviation of molecular area occurred at a lower PIN-a molar fraction than DPPC/PIN-a monolayers. The maximum difference between ideal mean molecular area of the mixed DPPG/PIN-a monolayer at 15 mN/m represented almost a factor of 2 at $X_{PIN-a} = 0.185$, whereas such a difference was observed at $X_{PIN-a} = 0.125$ for the DPPC/PIN-a mixed film. However, at below and above these X_{PIN-a} limiting values, the expansion induced by the protein was higher for the DPPG than for the DPPC monolayers.

Adsorption of PIN-a to DPPC and DPPG monolayers

The adsorption of PIN-a to phospholipid monolayers was studied in presence of zwitterionic (DPPC) and negatively charged phospholipids (DPPG) at different surface pressure. PIN-a solution was injected beneath the spread lipid monolayer kept under a defined initial surface pressure (5, 10, 15, 20, 25, 30, and 35 mN/m) at $X_{PIN-a} = 0.2$. The adsorption of PIN-a to the lipid film was accompanied by an increase of surface pressure. Table 1 shows that the increase of surface pressure due to the adsorption of PIN-a to the lipid monolayer was greater with lower initial pressure of the lipid film. The increase of surface pressure due to the adsorption of PIN-a was greater in the presence of negatively charged DPPG than with zwitterionic DPPC. The critical pressure which is the value of initial pressure beyond which there is no increase in surface pressure was ~25 mN/m and 35 mN/m for DPPC and DPPG, respectively.

Effect of PIN-a on the structure and organization of DPPC monolayers

To study the effect of PIN-a on the structure and organization of phospholipid monolayers, PIN-a was injected beneath a preformed lipid monolayer containing 5 mol % BODIPY and compressed to 15 mN/m. The dark and bright regions of the DPPC monolayer displayed identical shapes with the LC and LE phases, respectively, that have been described for other fluorescent lipid probes such as Rh-DPPE (Disher et al., 1999), NBP-PC (Taneva and Keough, 2000; Ruano et al., 1998), and SR-DPPE (Signor et al., 1994). Therefore, the fluorescent BODIPY probe was actually excluded from the condensed phases although it was not covalently bound to a phospholipid molecule. Furthermore, no significant effect of the fluorescent probe on the π-A isotherm of DPPC was noticed (results not shown).

TABLE 1 Values of the overpressure ($\Delta\pi$) measured in the film DPPC and DPPG versus the initial pressure of the monolayers (π_i) , 2 h after the injection of the PIN-a in the subphase; $X_{PIN-a} = 0.2$

π_i (mN/.m)	DPPC $\Delta\pi$ (mN/m)	DPPG $\Delta\pi$ (mN/m)
5	10.3	11.0
10	7.2	8.9
15	5.7	6.7
20	1.7	6.8
25	0.5	3.6
30		2.5
35		1.1

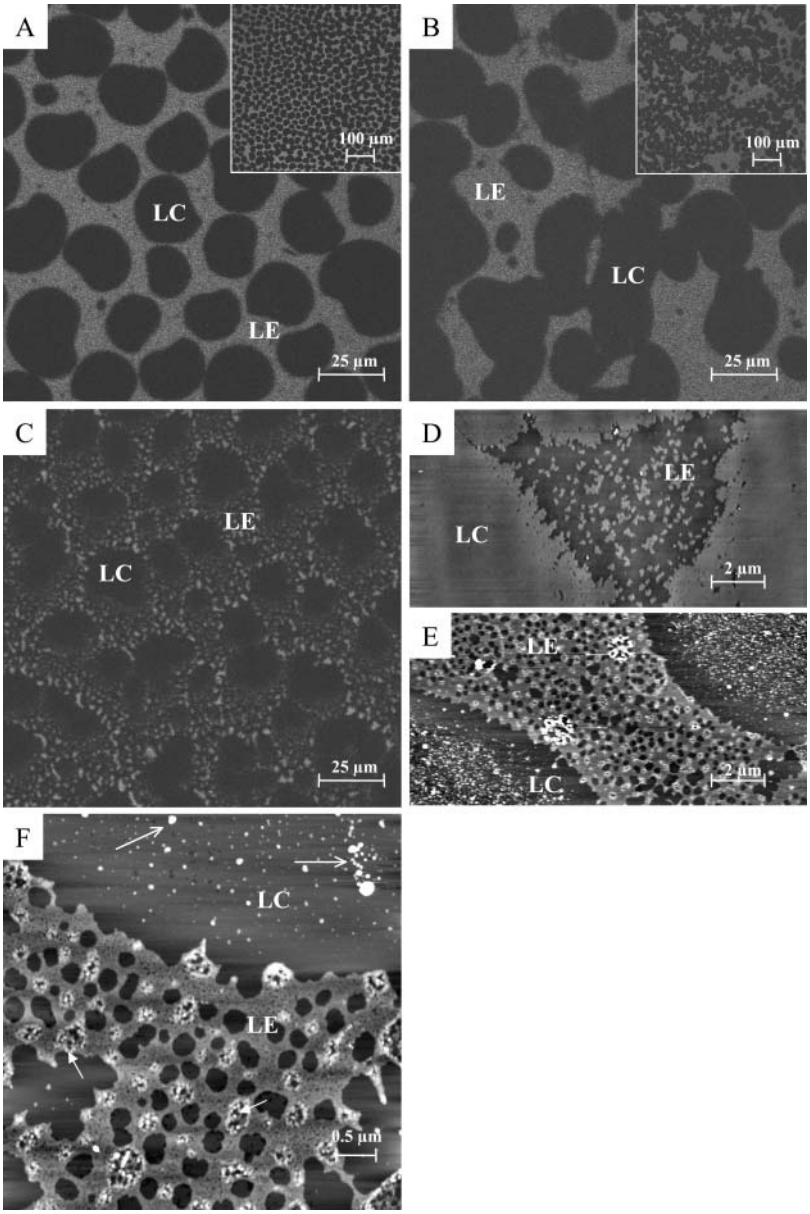

FIGURE 3 CLSM and AFM images of DPPC monolayer (π_i = 15 mN/m) before and after the injection of PIN-a into the subphase of the monolayer. (*A–C*) CLSM images of DPPC monolayer during the PIN-a injection experiments. (*A*) DPPC/5 mol % BODIPY monolayer before PIN-a injection transferred at π = 15 mN/m to a mica substrate. The dark regions are liquid-condensed (LC) domains that exclude the fluorescent probe. The LC domains are dispersed homogeneously in the LE phase. (*B*) DPPC/5 mol % BODIPY monolayer, 2 h after the injection of PIN-a, transferred at π_{2h} = 21 mN/m. The LC domains coalesced with each other to form long domains. Large areas of the liquid phase appeared devoid of LC domains. (*C*) DPPC monolayer, 2 h after the injection of PIN-a/5 mol % rho-PIN-a, transferred at π_{2h} = 21 mN/m. PIN-a is localized in the LE phase of the DPPC monolayer. (*D–F*) AFM images of DPPC monolayer during the PIN-a injection experiments. (*D*) DPPC monolayer before injection of PIN-a transferred at π_i =15 mN/m to a mica substrate. The LC domains are light gray, whereas the dark gray regions represent the LE phase. (*E*) DPPC monolayer, 2 h after the injection of PIN-a, transferred at π_{2h} = 21 mN/m. In the presence of PIN-a, the phase image displays contrast inversion due to the difference in height of the LC domains to the LE phase. (*F*) Higher magnification of the DPPC monolayer after PIN-a insertion. A thick network with large aggregates is observed in the LE phase (*plain arrows*) whereas numerous small globular protrusions are observed in the LC domains (*opened arrow*). The *z*-scale is 10 nm for all AFM images.

The laser confocal image reported in Fig. 3 *A* shows the monolayer of DPPC-BODIPY compressed at an initial surface pressure of 15 mN/m and equilibrated for 3 h before transfer onto the solid mica substrate. The black nonfluorescent domains (LC phase) were dispersed very homogeneously in a fluorescent environment (LE phase; see Fig. 3 *A*, *inset*). The condensed domains with a size close to 25 μm displayed a kidney-bean shape in agreement with previous observations (Nag et al., 1991; Perez-Gil et al., 1992). The laser confocal image presented in Fig. 3 *B* shows the DPPC-BODIPY monolayer, 2 h after the injection of PIN-a beneath the monolayer, with a final surface pressure of the monolayer close to 21 mN/m. The distribution and shape of condensed domains changed. The LC domains coalesced to form larger areas heterogeneously dispersed in the LE phase (see Fig. 3 *B*, *inset*).

The localization of PIN-a in the DPPC monolayer was studied by using a PIN-a solution containing 5 mol % of PIN-a labeled with fluorescent rhodamine (rho-PIN-a). The conditions of preparation of the DPPC monolayer (π_i = 15 mN/m) and of injection of the fluorescent labeled PIN-a (π_{2h} = 21 mN/m) were as described for the experiments performed with nonlabeled PIN-a. The rho-PIN-a gave rise to a π-A isotherm strictly identical to that of nonconjugated PIN-a (results not shown). In Fig. 3 *C*, the protein fluorescence was distributed in the film as small bright spots surrounded by a nonfluorescent black matrix. The black matrix can form large circular zones with a diameter from 10

μm to >30 μm, quite similar to the LC phase observed with the BODIPY labeling (see Fig. 3 *B*). Therefore, the protein fluorescence was mainly located in the LE phase.

At the nanometer resolution of AFM, more detailed features of the lipid monolayer in presence or absence of PIN-a can be highlighted. Fig. 3 *D* shows an AFM image (15 μm $\times$ 7.5 μm) of a DPPC monolayer imaged that was previously observed by CLSM (see Fig. 3 *A*). This image clearly shows two distinct height areas. The higher regions are brighter and can be designated the LC phase, whereas the darker regions represent the fluid LE phase. These LC and LE phases have been previously described (Yang et al., 1995; Hollars and Dunn, 1998; Vié et al., 2000; Krol et al., 2000) and such a conclusion was in agreement with our observations in CLSM. Using AFM, the height difference between the LC domains and the LE phase was measured and a value of 1.2 $\pm$ 0.2 nm was obtained for a monolayer compressed at 15 mN/m, in agreement with data obtained ($\sim$1 nm) on DPPC/DPPG monolayer transferred at the same surface pressure (Krol et al., 2000). However, the dark LE phase contained smaller bright LC domains ($\sim$0.2-μm diameter) which were aggregated at the periphery of the larger bright LC domains. Although the large LC domains were easily observed in CLSM (see Fig. 3 *A*) the small ones could not be highlighted because of the lower resolution of CLSM vs. AFM. The origin of these small LC domains dispersed in the LE phase remains unclear. It has been suggested that either there is a real coexistence of these small LC domains and the LE phase in the lipid monolayers (Chi et al., 1993; Yang et al., 1995) or that these small domains would be artifactually introduced on transfer of the monolayer on the solid support (Fang and Knobler, 1995; Santesson et al., 1995; Sikes and Schwartz, 1997; Hollars and Dunn, 1998; Shiku and Dunn, 1998).

Fig. 3 *E* (7.5 μm $\times$ 15 μm) and *F* (5 μm $\times$ 5 μm) represents AFM images obtained 2 h after the injection of PIN-a beneath the DPPC monolayer, the experimental conditions being identical to those described for Fig. 3 *C*. In presence of PIN-a, the image displayed a contrasted inversion in the difference of height between the large circular LC domains and the surrounding matrix. The circular domains appeared darker than the background. In Fig. 3 *F*, the presence of a thick network with large aggregates in the background could indicate that the PIN-a was inserted mainly in areas identified as the LE phase with BODIPY labeling. The apparent difference of height between LE and LC phases can be measured by AFM and the value is 1.7 $\pm$ 0.2 nm. This showed that the fluid phase has increased in thickness by 2.9 nm in presence of PIN-a compared to the DPPC alone. These aggregates corresponded probably to PIN-a aggregates (see Fig. 3 *F*, *plain arrow*) localized as fluorescent domains in the LE phase of DPPC by confocal microscopy (see Fig. 3 *C*). Furthermore, the LC domains of DPPC contained numerous and small globular protrusions (see Fig. 3, *E* and *F*, *open arrow*) which could also correspond to the insertion of small PIN-a aggregates. These globular structures in the LC domains were too small (60–300 nm) to be observed at the resolution level of confocal microscopy.

Effect of PIN-a on the structure and organization of DPPG monolayer

A representative CLSM image of DPPG-BODIPY monolayer (π_i = 15 mN/m) is presented in Fig. 4 *A*. Before injection of PIN-a, the black condensed domains of DPPG were dispersed homogeneously in the fluorescent LE phase (see *inset*, Fig. 4 *A*). The mean size of the condensed domains was $\sim$15 μm. The CLSM image presented in Fig. 4 *B* shows the structure and organization of the DPPG-BODIPY monolayer, 2 h after the injection of PIN-a beneath the monolayer, with a final surface pressure of the monolayer close to 22 mN/m. Upon insertion of PIN-a, an heterogeneous size distribution of the condensed domains was observed with many small domains close to 5 μm. Fig. 4 *C* shows the DPPG-PIN-a mixed monolayer at identical initial and final surface pressure using the fluorescent rho-PIN-a probe. Comparing Fig. 4, *B* and *C*, the fluorescence of rho-PIN-a was observed homogeneously in the BODIPY-rich area formed by DPPG in LE phase. In Fig. 4 *C*, interestingly, rho-PIN-a appeared also in LC domains where they formed conical-shape areas (CSAs).

AFM images confirmed the presence of conical shape inclusions in the LC domains of the DPPG monolayer after injection of PIN-a. In Fig. 4 *D*, one can note that these CSAs were less numerous and smallest at the periphery of LC domains in agreement with the low protein fluorescent signal detected by CLSM in that peripheral zone (Fig. 4 *C*). CSAs were heterogeneous in size and regularly dispersed in the LC domains of the DPPG monolayer. Fig. 4 *E* shows an AFM image (10 μm $\times$ 5 μm) of DPPG monolayer in absence of PIN-a. The phase separation at π = 15 mN/m was observed and the LE phase of DPPG did not contain small LC domains as it was described for DPPC at this surface pressure. A height difference of 2 $\pm$ 0.2 nm was observed between the LE and LC phase of the DPPG monolayer. Fig. 4 *F* presents the circular LC domain and the fluid phase domain in a DPPG/PIN-a monolayer at the same magnification as shown in Fig. 4 *E*. In presence of PIN-a, the LE and LC domains of DPPG were still dark and bright, respectively. In this case, a height difference of 1.1 $\pm$ 0.2 nm was observed between LC and LE phases. In contrast with what it was observed with DPPC, no height inversion was observed in the presence of PIN-a. This suggested that PIN-a could be localized in the dark zones of the LE phase and of CSAs dispersed in the LC phase. In Fig. 4 *G*, it was also observed that the adsorption of PIN-a led to very numerous and small LC domains uniformly partitioned in the LE phase. Fig. 4, *I* and *J*, show that the CSAs found in the LC domains of DPPG/PIN-a monolayer contained small LC domains in

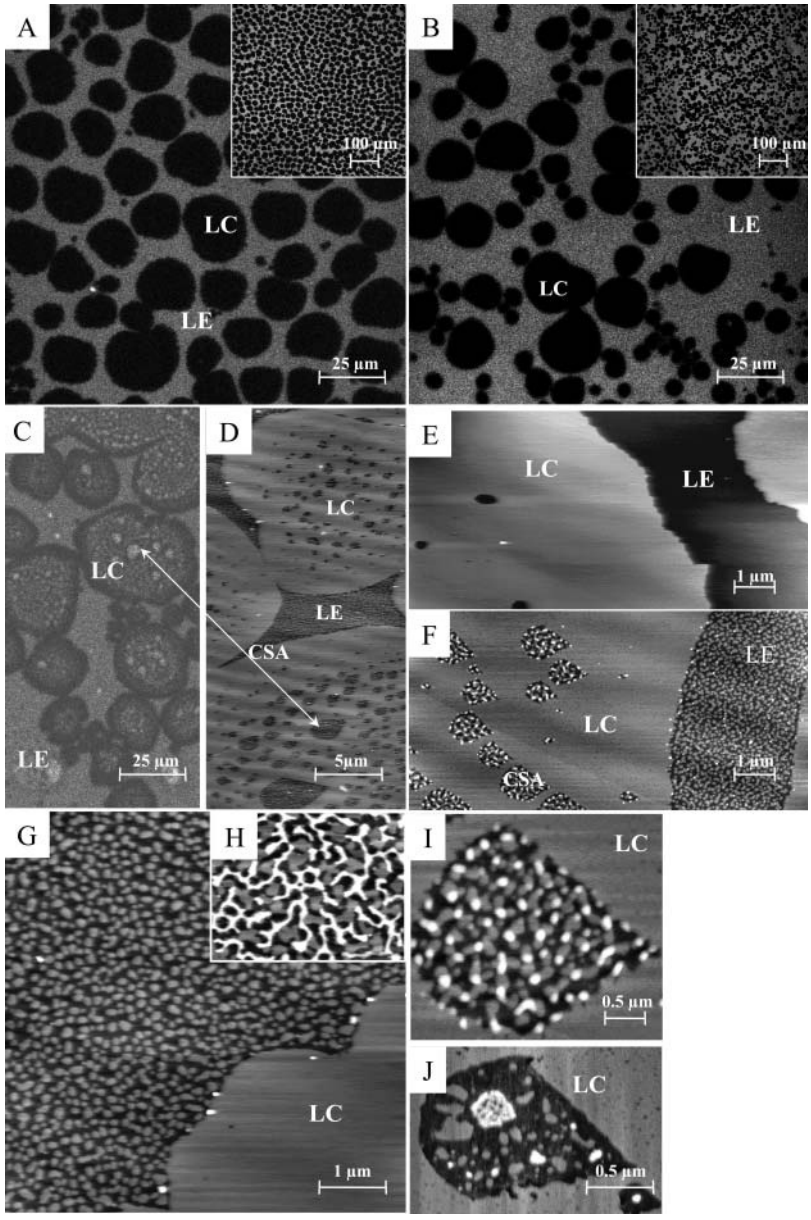

FIGURE 4 CLSM and AFM images of DPPG monolayer (π_i = 15 mN/m) before and after the injection of PIN-a. (*A–C*) CLSM images of DPPG monolayer during the PIN-a injection experiments. (*A*) DPPG/5 mol % BODIPY monolayer before injection of PIN-a transferred at π = 15 mN/m to a mica substrate. (*B*) DPPG/5 mol % BODIPY monolayer, 2 h after the injection of PIN-a in the subphase, transferred at π_{2h} = 22 mN/m. (*C*) DPPG monolayer, 2 h after the injection of PIN-a/5 mol % rho-PIN-a in the subphase, transferred at π_{2h} = 22 mN/m. PIN-a is localized both in the LC domains and in the LE phase. (*E*) DPPG monolayer before injection of PIN-a in the subphase, transferred at π_i =15 mN/m. The liquid-expanded phase (LE) did not contain small LC domains as it was described for DPPC. (*D–F*) DPPG monolayer, 2 h after the injection of PIN-a in the subphase (π_f = 22 mN/m). LC domains contain regularly dispersed conical shape areas (*CSA*). The material contained in the CSA appeared to be similar to the LE phase material. (*G–H*) Higher magnifications of the LE phase strewn with numerous small islands of LC phase. (*H*) Filament network (*white*) above the LE phase. (*I–J*) CSA, (*I*) globular protrusions (*white*) in CSA, and (*J*) large aggregate (*white*) observed in the middle of the CSA. The *z*-scale is 5 nm for all AFM images.

a more fluid phase. Finally, the insertion of PIN-a in the LE phases inducing an increase of lateral pressure could be responsible for the condensation of the lipids in these phases. In contrast in the CSA, PIN-a seems to split the LC phase into smaller domains. In Fig. 4, *H* and *I*, white protrusions of higher height were observed, both in the LE phase and in the CSA. In a few places very localized on the sample the protrusions formed a network of interconnected filaments and globular structures. These protrusions could correspond to PIN-a aggregates.

We also studied the insertion of PIN-a in a DPPG monolayer compressed at a higher surface pressure (π_i = 25 mN/m). At this surface pressure, the insertion of PIN-a in the DPPG monolayer led to an overpressure ~3 mN/m. Fig. 5 *A* shows an AFM image (25 μm × 12.5 μm) of DPPG monolayer before injection of PIN-a compressed to 25 mN/m. At this surface pressure, only the condensed phase was observed for the lipid monolayer. Fig. 5 *B* represents an AFM image (25 μm × 12.5 μm) of the DPPG monolayer, 2 h after the injection of PIN-a, where domains of different height are evident. At higher magnification, in Fig. 5 *C*, it was observed that the higher domains formed a network of filaments. These filaments were 0.9 ± 0.2 nm higher than the lower part of the film, a value close to that obtained for the PIN-a insertion in the DPPG monolayer compressed initially at 15 mM/m. Zooming on this network, in Fig. 5 *D*, showed that the long filaments were composed by aggregation of globular structures with a diameter close to 15 ± 0.2 nm. Fig. 5 *E* shows that such globular units displayed similar diameter in the aggregates observed after

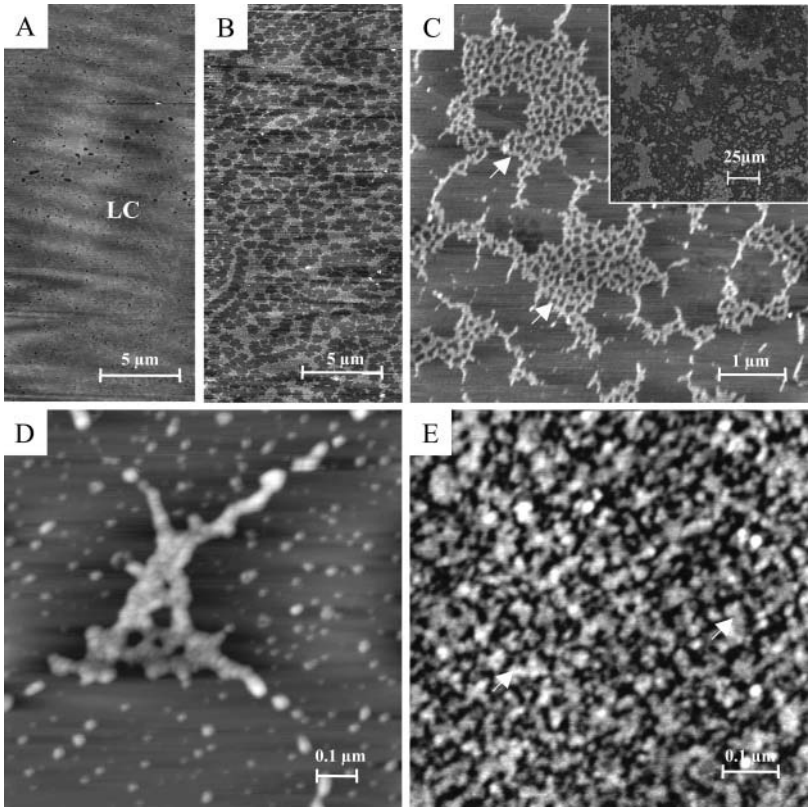

FIGURE 5 AFM images of DPPG monolayer ($\pi_i = 25$ mN/m) before and after the injection of PIN-a into the subphase of the monolayer. (*A*) DPPG monolayer before injection of PIN-a compressed to 25 mN/m. The lipid is exclusively in condensed phase. (*B–D*) DPPG monolayer, 2 h after the injection of PIN-a. (*B*) AFM image provides direct evidence for the formation of a network inserted in the condensed DPPG monolayer. (*C*) Arrows indicate protein aggregates. Inset in *C* corresponds to CLSM image of DPPG monolayer at 25 mN/m in presence of rho-PIN-a. (*D*) Higher magnification of aggregated protrusions (*white*) in the LC phase of DPPG. (*E*) AFM image of PIN-a monolayer transferred at 14 mN/m. The *z*-scale is 5 nm for *A–C* and 10 nm for *D–E* images.

adsorption of the protein alone at $\pi = 14$ mN/m. Finally, the observations done by CLSM at the same surface pressure (25 mN/m) using rho-PIN-a showed that the protein is heterogeneously dispersed in the monolayer, forming relatively large domains (see *inset*, Fig. 5 *C*). In most cases, the size of these protein domains is well above that of the filament network observed by AFM. From a comparison of AFM and CLSM data, we can suggest that the protein could be both adsorbed under the DPPG film (CLSM) and could penetrate the monolayer where it formed an aggregated network.

DISCUSSION

Lipid monolayers are interesting model systems to explore the role of lipid-protein interactions in the function and organization of cell membranes (Brockman, 1999; Maget-Dana, 1999) as well as in the formation and stability of food interfaces, e.g., foams and emulsions (Mackie et al., 1999). Furthermore, the structure and organization of the lipoprotein monolayers can be easily investigated by coupling Langmuir-Blodgett and imaging techniques (Hollars and Dunn, 1998). For the first time, we have applied such an approach to puroindolines, wheat seed proteins whose interfacial properties are related to both their biological and technological functions (Douliez et al., 2000). In this study, we have chosen two synthetic phospholipids, DPPC and DPPG, which permits the observation of both LE and LC phases at a surface pressure and the exploration of the electrostatic contribution in the lipid-protein interactions. Fundamental information on the behavior of the protein at such model lipid interfaces was essential to obtain before undertaking the exploration of the interactions of puroindolines with more relevant membrane and food phospholipids.

The π-A isotherms of mixed PIN-a/phospholipid monolayers show three distinct regions corresponding: 1), to the phase transition of the pure lipids (4–5 mN/m for DPPC and 10 mN/m for DPPG); 2), to the phase transition of PIN-a (12.5 mN/m); and 3), to a transition (30 mN/m) specific to the mixed lipid-protein system. Beyond the latter transition, the coincidence of the isotherms of mixed DPPC/PIN-a and pure DPPC monolayers suggests that the protein is expelled from the lipid monolayer into the subphase. On the contrary, the higher molecular area of DPPG/PIN-a monolayers at >30 mN/m than for pure DPPG suggests that squeezing PIN-a out of the DPPG monolayer is not completed. Upon mixing PIN-a with DPPC and DPPG, the mean molecular area measured at 15 mN/m shows a positive deviation far from an additive behavior of the isolated lipid and protein. This nonideal mixing is more significant for DPPG than for DPPC monolayers. These results show that PIN-a interacts with both synthetic phospholipids and displays a higher affinity for DPPG than for DPPC. Similar conclusions arise from adsorption experiments where the critical surface pressure for the adsorption of PIN-a is higher for DPPG (35 mN/m) than for DPPC (25 mN/m) monolayers. The

monolayer experiments confirm previous results obtained on lipid bilayers composed by synthetic phospholipids and wheat polar lipids (Dubreil et al., 1997; Le Guernevé et al., 1998). PIN-a contains an amphiphilic and cationic tryptophan-rich domain (Trp-Arg-Trp-Trp-Lys-Trp-Trp-Lys), which is probably involved in the interaction with the hydrophilic glycerol backbone, acyl chain, and negatively charged phosphate group of the phospholipids as observed in membrane proteins (Killian and von Heijne, 2000). Since PIN-a contains eight arginine and six lysine residues and displays a high net positive charge (+5), the overall electrostatic contribution in the lipid-protein interaction is significantly higher for DPPG than for DPPC. In a first attempt, both local (tryptophan-rich domain) and overall electrostatic contributions can potentiate the lipid-protein interactions and therefore promote insertion of the protein in condensed lipid monolayers and prevent protein from squeezing out of DPPG monolayers at high surface pressure.

Confocal laser scanning microscopy (CLSM) and atomic force microscopy (AFM) provides complementary information on the structure and organization of the phospholipid and phospholipid-protein monolayers that are related to the data obtained by monolayer experiments. The imaging experiments have been performed using PIN-a adsorption to phospholipid monolayers spread at initial surface pressures of 15 and 25 mN/m. At 15 mN/m, where both LE and LC phases are present, PIN-a adsorbs both to DPPC and DPPG monolayers whereas, at 25 mN/m where lipids are in the condensed state, significant adsorption occurs only to the DPPG monolayer. By CLSM, it is observed that, at an initial pressure of 15 mN/m, PIN-a partitions in the LE phase of DPPC and induces the coalescence of the LC domains. By AFM it is observed that PIN-a self-associates in the fluid LE phase to form large aggregates that are probably responsible for the increase of the thickness of this LE phase. In AFM, small globular protrusions (60–300 nm) are observed within the large condensed domains of DPPC. These small protrusions, not observed at the limited resolution of CLSM, could correspond to small PIN-a aggregates that are not totally excluded from the LC phase of DPPC. Furthermore, the pure protein spontaneously spreads at the air-water interface where AFM reveals the formation of a highly and heterogeneously aggregated film. Therefore, we suggest that PIN-a adsorbs at the air-water interface where protein aggregates and then penetrates the loosely packed regions of the lipid monolayer. Since experiments are performed near the saturation of the lipid binding sites of PIN-a, some protein aggregates are available to rearrange and penetrate the more condensed domains of the DPPC monolayer. Such a mechanism can account for the weak effect of PIN-a on the gel-fluid phase transition of dimyristoylphosphatidylcholine bilayers (Le Guernevé et al., 1998).

In the case of a DPPG/PIN-a monolayer spread at an initial pressure of 15 mN/m, fluorescent microscopy reveals that PIN-a splits larger LC domains into smaller ones. The protein is located both in the LE phase and in the LC domains of DPPG monolayer. PIN-a forms conical shape areas (CSAs) in the condensed domains. Detailed structure of CSAs provided by AFM images suggest that they contain both PIN-a aggregates and small condensed lipid domains in a fluider phase. Furthermore, in presence of PIN-a, the LE phase of the DPPG is strewed with small numerous islands of condensed lipids. The presence of these small condensed domains confirms the splitting of the LC domains into smaller ones that is observed by CLSM. Therefore, interaction of the positively charged PIN-a with negatively charged DPPG induces a significant rearrangement of the condensed domains at both the micron and nanometer scales. Such effects that occur at a protein molar fraction ($X_{\text{PIN-a}} = 0.2$) close to the saturation of the binding site (Wilde et al., 1993; Dubreil et al., 1997) could account for the suppression of the gel-fluid phase transition of dimirystoylphosphatidylglycerol bilayers observed at this lipid-protein ratio (Le Guernevé et al., 1998).

When the DPPG monolayer is initially compressed at 25 mN/m, AFM imaging shows that the protein is capable of penetrating the highly condensed lipid phase where it forms an aggregated network. CSAs are no longer observed at this high surface pressure. Furthermore, it is observed by the CLSM that the protein is adsorbed to the condensed monolayer, where it forms heterogeneously dispersed domains with a surface area well above the surface area covered by the aggregated PIN-a network highlighted by AFM. Therefore, at this surface pressure only a part of the aggregated protein is capable of penetrating the monolayer. It can be suggested that with increasing surface pressure, the high lipid packing promotes the self-aggregation of the protein adsorbed at the polar interface of the lipid monolayer. Afterwards, some of the protein aggregates can insert into the monolayer where they rearrange in a protein network and not in CSA. The interactions between the lipids and the aggregated protein leads to the formation of a very stable lipoprotein film that can be observed above 30 mN/m in compression isotherms.

Finally, the PIN-a adsorption experiments realized in DPPC and DPPG monolayers, at different surface pressure, suggest that the degree of penetration of PIN-a in the phospholipid monolayers is probably related to the aggregation properties of PIN-a. Aggregation of the protein is driven by the charge of the lipid headgroups and lipid packing. Furthermore, AFM images of puroindoline monolayer shows that the protein alone is capable of forming highly aggregated films at the air-water interface. Desorption of proteins from foam films is generally promoted through competition with more surface-active molecules such as polar lipids and surfactants (Dickinson and Woskett, 1989). On the contrary, puroindoline foams are resistant to destabilization and display in some cases enhancing foaming properties in the presence of surface-active molecules (Wilde et al., 1993; Dubreil et al., 1997). Therefore, the aggregation

state of puroindolines and puroindoline-lipid complexes at air-water interface probably account for the unique foaming properties of these proteins.

From a biological standpoint, our results demonstrate that PIN-a interferes on the lipid-lipid interactions within membranes since it can penetrate a phospholipid monolayer at a surface pressure close to the surface pressure, i.e., 30–45 mN/m, estimated for the biological membrane (Demel et al., 1975; Feng, 1999; Nagle, 1976). This property probably accounts for the antimicrobial properties of puroindolines (Dubreil et al., 1998a). In this regard, recent studies have demonstrated that puroindolines form ion channels in membranes (Charnet et al., 2003). Our results suggest that the permeability changes could be due mainly to changes in the lipid packing induced by the protein aggregates in the membrane. The relatively high puroindoline concentrations needed to observe ion channel activity (Charnet et al., 2003) and inhibition of fungal growth (Dubreil et al., 1998a) could be related to the necessity of the formation of protein aggregates for the expression of these biological properties. In any cases, we do not observe formation of organized protein oligomers in the lipid monolayer as described for pore-forming peptides and proteins (Diociaiuti et al., 2002; Müller et al., 2002). However, the phospholipids used here and in previous ion-channel experiments (Charnet et al., 2003) are different and, as mentioned above, the nature of the lipid used can impose a significant drawback on the aggregation state of the puroindoline in the lipid film. Therefore, it clearly appears that it should be essential to further study the relationship between the lipid composition and the aggregation properties of puroindolines at the lipid-water interface.

Brigitte Bouchet is acknowledged for her valuable assistance in confocal microscopy and André Lelion for his technical assistance in protein purification.

This work was supported by grants from Region Bretagne and Pays de la Loire. L.D. received a postdoctoral fellowship from Region Bretagne.

REFERENCES

Biswas, S. C., L. Dubreil, and D. Marion. 2001a. Interfacial behaviour of wheat puroindolines: monolayers of puroindolines at the air-water interface. *Coll. Polym. Sci.* 279:607–614.

Biswas, S. C., L. Dubreil, and D. Marion. 2001b. Interfacial behaviour of wheat puroindolines: study of adsorption at the air-water interface from surface tension measurement using Wilhelmy plate method. *J. Coll. Interf. Sci.* 244:245–253.

Blochet, J. E., C. Chevalier, E. Forest, E. Pebay-Peyroula, M. F. Gautier, P. Joudrier, M. Pézolet, and D. Marion. 1993. Complete amino acid sequence of puroindoline, a new basic and cystein rich protein with a unique tryptophan-rich domain, isolated from wheat endosperm by Triton X-114 phase partitioning. *FEBS Lett.* 329:336–340.

Brockman, H. 1999. Lipid monolayers: why use half a membrane to characterize protein-membrane interactions? *Curr. Opin. Struct. Biol.* 9:438–443.

Charnet, P., G. Molle, D. Marion, M. Rousset, and V. Lullien-Pellerin. 2003. Puroindolines form ion channels in biological membranes. *Biophys. J.* 84:2416–2426.

Chi, L. F., M. Anders, H. Fuchs, R. R. Johnston, and H. Ringsdorf. 1993. Domain structures in Langmuir-Blodgett films by atomic force microscopy. *Science.* 259:213–216.

Clark, D. C., P. J. Wilde, and D. Marion. 1994. The protection of beer foam against lipid induced destabilization. *J. Inst. Brew.* 100:23–25.

Demel, R. A., W. S. Geurts van Kessel, R. F. Zwaal, B. Roelofsen, and L. L. van Deenen. 1975. Relation between various phospholipase actions on human red cell membranes and the interfacial phospholipid pressure in monolayers. *Biochim. Biophys. Acta.* 406:97–107.

Dickinson, E., and C. M. Woskett. 1989. Competitive adsorption between proteins and small-molecule surfactants in food emulsions. *In* Food Colloids. R. B. Bee, J. Mingins, and P. Richmond, editors. Royal Society of Chemistry, London, UK pp.74–96.

Diociaiuti, M., F. Bordi, A. Motta, A. Carosi, A. Molinari, G. Arancia, and C. Coluzza. 2002. Aggregation of gramicidin A in phospholipid Langmuir-Blodgett monolayers. *Biophys. J.* 82:3198–3206.

Disher, B. M., W. R. Schief, V. Vogel, and S. H. Hall. 1999. Phase separation in monolayers of pulmonary surfactant phospholipids at the air-water interface: composition and structure. *Biophys. J.* 77:2051–2061.

Douliez, J. P., T. Michon, K. Elmorjani, and D. Marion. 2000. Structure, biological and technological functions of lipid transfer proteins and indolines, the major lipid binding proteins from cereal kernels. *J. Cereal Sci.* 32:1–20.

Dubreil, L., J. P. Compoint, and D. Marion. 1997. Interactions of puroindolines with wheat flour polar lipids determine their foaming properties. *J. Agric. Food Chem.* 45:108–116.

Dubreil, L., T. Gaborit, B. Bouchet, D. Gallant, W. Broekaert, L. Quillien, and D. Marion. 1998a. Spatial and temporal distribution of the major isoforms of puroindolines (puroindoline-and puroindoline-b) and a non-specific lipid transfer protein (ns-LTPe1) of *Triticum aestivum* seeds. Relationships with their in vitro antifungal properties. *Plant Sci.* 138:121–135.

Dubreil, L., S. Méliande, H. Chiron, J. P. Compoint, L. Quillien, G. Branlard, and D. Marion. 1998b. Effect of puroindolines on the bread-making properties of wheat flour. *Cereal Chem.* 75:222–229.

Dubreil, L., S. C. Biswas, and D. Marion. 2002. Localization of puroindoline-a and lipids in bread dough using confocal laser microscopy. *J. Agric. Food Chem.* 50:6078–6085.

Fang, J., and C. M. Knobler. 1995. Control of density in self-assembled organosilane monolayers by Langmuir-Blodgett deposition. *J. Phys. Chem.* 99:10425–10429.

Feng, S. S. 1999. Interpretation of mechanochemical properties of lipid bilayer vesicles from the equation of state or pressure area measurement of the monolayer at the air-water interface or oil-water interface. *Langmuir.* 15:998–1010.

Gaines, G. L. 1966. Mixed monolayers. *In* Insoluble Monolayers at Liquid-Gas Interfaces. E. Prigogine, editor. Interscience, New York. pp.281–300.

Hollars, C. W., and R. C. Dunn. 1998. Submicron structure in L-α-dipalmitoylphosphatidylcholine monolayers and bilayers probed with confocal, atomic force, and near-field microscopy. *Biophys. J.* 75:342–353.

Husband, F., P. J. Wilde, D. Marion, and D. C. Clark. 1994. A comparison of the foaming and interfacial properties of two related lipid binding proteins from wheat in the presence of a competitive surfactant. *In* Food Macromolecules and Colloids. E. Dickinson, and D. Lorient, editors. Royal Society of Chemistry, London, UK. pp.285–296.

Killian, J. A., and G. von Heijne. 2000. How proteins adapt to a membrane-water interface. *Trends Biochem. Sci.* 25:429–434.

Krishnamurthy, K., C. Balconi, J. E. Sherwood, and M. J. Giroux. 2001. Wheat puroindolines enhance fungal disease resistance in transgenic rice. *Mol. Plant Microbe Interact.* 14:1255–1260.

Krol, S., M. Ross, M. Sieber, S. Künneke, H. Galla, and A. Janshoff. 2000. Formation of three-dimensional protein-lipid aggregates in monolayer films induced by surfactant protein B. *Biophys. J.* 79:904–918.

Le Bihan, T., J. E. Blochet, A. Désormeaux, D. Marion, and M. Pézolet. 1996. Determination of the secondary structure and conformation of puroindolines by infrared and Raman spectroscopy. *Biochemistry.* 35:12712–12722.

Le Guernevé, C., M. Seigneuret, and D. Marion. 1998. Interaction of the wheat endosperm lipid-binding protein puroindoline-a with phospholipids. *Arch. Biochem. Biophys.* 360:179–186.

Mackie, A. R., A. P. Gunning, P. J. Wilde, and V. J. Morris. 1999. Organic displacement of protein from the air-water interface by competitive adsorption. *J. Coll. Interf. Sci.* 210:157–166.

Maget-Dana, R. 1999. The monolayer technique: a potent tool for studying the interfacial properties of antimicrobial and membrane-lytic peptides and their interactions with lipid membranes. *Biochim. Biophys. Acta.* 1462:109–140.

Marion, D., and D. C. Clark. 1995. Wheat lipids and lipid binding proteins: structure and function. *In* Wheat Structure, Biochemistry and Functionality. J. D. Shofield, editor, Royal Society of Chemistry, London, UK. pp.245–260.

Mattei, C., K. Elmorjani, J. Mologo, D. Marion, and E. Benoit. 1998. The wheat proteins puroindoline-a and alpha1-purothionin induce nodal swelling in myelinated axons. *Neuroreport.* 9:3803–3807.

Minones, J., Jr., J. Minones, O. Conde, J. M. Rodriguez, and P. Dynarowicz-Latka. 2002. Mixed monolayers of amphotericin B-dipalmitoylphosphatidylcholine: study of complex formation. *Langmuir.* 18: 2817–2827.

Morris, C. F. 2002. Puroindolines: the molecular genetic basis of wheat grain hardness. *Plant Mol. Biol.* 48:633–647.

Müller, D. J., H. Janovjak, T. Lehto, L. Kuerschner, and K. Anderson. 2002. Observing structure, function and assembly of single proteins by AFM. *Prog. Biophys. Mol. Biol.* 79:1–43.

Nag, K., N. H. Rich, C. Boland, and K. M. W. Keough. 1991. Epifluorescence microscopic observation of monolayers of dipalmitoylphophatidylcholine: dependence of domain size on compression rates. *Biochim. Biophys. Acta.* 1068:157–160.

Nagle, J. F. 1976. Theory of monolayer and bilayer phase transitions: effect of headgroup interactions. *J. Membr. Biol.* 27:233–250.

Perez-Gil, J., K. Nag, S. Taneva, and K. M. W. Keough. 1992. Pulmonary surfactant protein SP-C causes packing rearrangements of dipalmitoylphosphatidylcholine in spread monolayers. *Biophys. J.* 63:197–204.

Ruano, M. L. F., K. Nag, L. A. Worthman, C. Casals, J. Perez-Gil, and K. M. W. Keough. 1998. Differential partitioning of pulmonary surfactant protein SP-A into regions of monolayers of dipalmitoylphosphatidylcholine and dipalmitoylphosphatidylcholine/dipalmitoylphosphatidylglycerol. *Biophys. J.* 74:1101–1109.

Santesson, L., T. M. H. Wong, M. Taborelli, P. Descouts, M. Liley, C. Duschl, and H. Vogel. 1995. Scanning force microscopy characterization of Langmuir-Blodgett films of sulfur-bearing lipids on mica and gold. *J. Phys. Chem. B.* 99:1038–1045.

Shiku, H., and R. C. Dunn. 1998. Direct observation of DPPC phase domain motion on mica surfaces under conditions of high relative humidity. *J. Phys. Chem. B.* 102:3791–3797.

Signor, G., S. Mammi, E. Peggion, H. Ringsdorf, and A. Wagenknecht. 1994. Interaction of Bombolitin III with phospholipid monolayers and liposomes and effect on the activity of phospholipase A2. *Biochemistry.* 33:6659–6670.

Sikes, H. D., and D. K. Schwartz. 1997. A temperature-dependent, two-dimensional condensation transition during Langmuir-Blodgett deposition. *Langmuir.* 13:4704–4709.

Subirade, M., C. Salesse, D. Marion, and M. Pézolet. 1995. Interaction of a nonspecific wheat lipid transfer protein with phospholipid monolayers imaged by fluorescence microscopy and studied by infrared spectroscopy. *Biophys. J.* 69:974–988.

Taneva, S. G., and K. M. W. Keough. 2000. Adsorption of pulmonary surfactant protein SP-A to monolayers of phospholipids containing hydrophobic surfactant protein SP-B or SP-C: potential differential role for tertiary interaction of lipids, hydrophobic proteins, and SP-A. *Biochemistry.* 39:6083–6093.

Vié, V., N. Van Mau, L. Chaloin, E. Lesniewska, C. Le Grimellec, and F. Heitz. 2000. Detection of peptide-lipid interactions in mixed monolayers, using isotherms, atomic force microscopy, and Fourier transform infrared analyses. *Biophys. J.* 78:846–856.

Wilde, P. J., D. C. Clark, and D. Marion. 1993. Influence of competitive adsorption of a lysopalmitoylphosphatidylcholine on the functional properties of puroindoline, a lipid binding protein isolated from wheat flour. *J. Agric. Food Chem.* 41:1570–1576.

Yang, X.-M., D. Xiao, Z.-H. Lu, and Y. Wei. 1995. Structural investigation of Langmuir-Blodgett monolayers of *L*-α-dipalmitoylphosphatidylcholine by atomic force microscopy. *Appl. Surf. Sci.* 90:175–183.